This is a repository copy of *Three-phase current-limiting droop controlled inverters operating in parallel*.

White Rose Research Online URL for this paper:
http://eprints.whiterose.ac.uk/144278/

Version: Accepted Version

eprints@whiterose.ac.uk
https://eprints.whiterose.ac.uk/

Three-Phase Current-Limiting Droop Controlled Inverters Operating in Parallel

Alexandros G. Paspatis and George C. Konstantopoulos
Dept. of Automatic Control and Systems Engineering
The University of Sheffield
Sheffield, UK
Email: {apaspatis1, g.konstantopoulos}@sheffield.ac.uk

Abstract—A new current-limiting droop controller is proposed in this paper for three-phase inverters operating in parallel. Droop control is employed to ensure the proportional power sharing between the parallel inverters while an inherent current-limiting property is achieved through the control design. The current limitation is mathematically proven using nonlinear analysis of the closed-loop system which leads to the boundedness of each inverter current under a threshold value at all times. Furthermore, small-signal analysis is performed to examine the closed-loop system stability of two parallel inverters equipped with the proposed controller. The example of two parallel inverters is further exploited to validate the proposed controller through Matlab/Simulink simulation results.

Index Terms—Parallel operation, proportional power sharing, current-limiting property, stability analysis, nonlinear control.

I. INTRODUCTION

Microgrids have gained attention in the last decade due to the rising integration of distributed energy resources (DERs) to the grid [1], [2]. The intelligent operation of microgrids is based on their control system which aims to solve issues such as power sharing, voltage and frequency regulation or islanding procedures. Control approaches are either designed in a distributed manner or through central controllers; however for each case, the stability of microgrids becomes a crucial aspect in the absence of a stiff grid that stabilizes voltage and frequency [3], [4].

Parallel operation of inverter-interfaced DERs is associated with the need of power sharing so that all the units are equally stressed and circulating currents are reduced. This is an important feature of the wider smart inverter concept as well [5]. The most common control approach that one can meet in microgrids is droop control [6], [7]. Droop control has the ability to share real and reactive power among DERs without requiring any communication. This plug-and-play feature has driven researchers to continuously improve its capabilities and application range [8]. Specifically, a lot of research is emphasizing on improving droop control functionality when inverters are facing different types of output impedance, suffering from extreme loading or experiencing voltage drops. Especially the issue of different type of output impedance, may lead to inaccurate real or reactive power sharing and many works have revisited the droop control design to address this issue.

In [9], a universal droop controller has been proposed which can achieve accurate power sharing for both real and reactive power regardless from the nature of the output impedance seen from each DER.

When a DER unit is connected to a stiff grid, a relatively constant voltage and frequency can be assumed at the PCC which may facilitate the stability analysis. However in the microgrid concept, due to the absence of synchronous generation with large capacity, stability issues become crucial since load voltage and frequency are governed from each DER. Hence, the control system of each DER needs to be analytically examined through a detailed stability analysis [10], [11]. The most commonly employed method to examine stability is the root-locus analysis of the linearized system, also known as the small-signal model stability analysis [12]–[15].

Apart from power sharing and stability properties, in order to increase autonomy and self-protection, a current-limiting property is required from every inverter control system [16], [17]. Conventional techniques include either a saturated PI controller or a switching to a different control scheme when faulty or overloading conditions appear [18], [19]. However, as highlighted in [18] and [19], both saturation units and switching between different dynamic controllers can lead to latch-up and wind-up which can eventually lead to instability. To overcome this issue, advanced current-limiting techniques have recently been proposed in [20] and [18] based on the concept of adding through the control design a virtual resistance or a virtual impedance. These techniques employ a current-limiting virtual impedance additionally to the nominal when the current limit is reached. Recently, in [21], a current-limiting droop controller has been designed that can offer a guaranteed current limitation at all times while this current limitation is inherently applied through the droop control loop, by using the bounded integral control (BIC) structure [22]. Nevertheless, in [21], the system under consideration consists of a single-phase grid-connected inverter while its functionality in case of inverters operating in parallel is still left to be proven.

In this paper the current-limiting droop control concept from [21] is proposed for three-phase inverters operating in parallel. To accomplish this, a new controller is proposed in the synchronous reference frame (SRF) to reduce the compu-
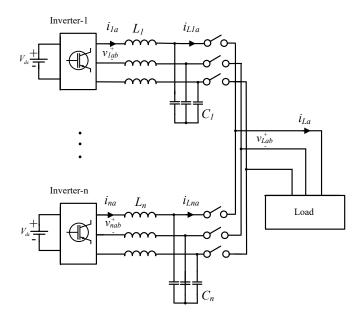
Fig. 1. n three-phase inverters connected to a common load through LC filters

tational burden and at the same time facilitate the controller analysis. The current-limiting property is proven through non-linear analysis of the closed-loop system which leads to the limitation of each inverter current under a threshold value at all times, even under transients. This current limitation is inherently applied to a droop controller that further guarantees the proportional power sharing between multiple inverters. Moreover, the small-signal model of the closed-loop system is developed in order to evaluate the stability properties of two paralleled three-phase inverters equipped with the proposed controller. The proposed control approach is verified through extended simulation results.

The paper is organized as follows. In Section II, the research problem is stated. In Section III, the proposed control strategy is presented while in Section IV, the current-limiting property is proven and the small-signal model stability is presented. In Section V, simulation results of two three-phase inverters operating in parallel are provided while in Section VI, the conclusions derived from this work are given.

II. SYSTEM MODELING AND PROBLEM FORMULATION

The system under consideration consists of n three-phase inverters operating connected to a common load bus through an LC filter, as depicted in Fig. 1. The inductance of the filter is denoted as L_i, with its parasitic resistance being ignored due to its small value, while the filter capacitor is denoted as C_i where i denotes the number of the inverter with $i \in [1, \ldots, n]$. The inverter voltage in the natural reference framework is denoted as v_{iabc} and the inverter current is given as i_{iabc} while the load voltage and current are denoted as v_{Labc} and i_{Labc}, respectively. The contribution to the total load current from each inverter is given as i_{Liabc}. Following the synchronous reference frame theory proposed in [23] and

thoroughly presented in [24], the $abc/dq0$ transformation is described from the matrix

$$T_{\alpha\beta} = \frac{2}{3} \begin{bmatrix} \sin\theta_a & \sin(\theta_a - 120) & \sin(\theta_a + 120) \\ \cos\theta_a & \cos(\theta_a - 120) & \cos(\theta_a + 120) \\ 0.5 & 0.5 & 0.5 \end{bmatrix},$$

where θ_a is the angle between phase a and the α axis, followed by the rotating transformation

$$T_{dq} = \begin{bmatrix} \cos\theta_i & \sin\theta_i \\ -\sin\theta_i & \cos\theta_i \end{bmatrix},$$

where θ_i is the angle of each inverter. The dynamic equations for any of the n parallel three-phase inverters in the dq framework can be written as

$$L_i \frac{di_{id}}{dt} = v_{id} - v_{Lid} + \omega_i L_i i_{iq} \tag{1}$$

$$L_i \frac{di_{iq}}{dt} = v_{iq} - v_{Liq} - \omega_i L_i i_{id} \tag{2}$$

$$C_i \frac{dv_{Lid}}{dt} = i_{id} - i_{Lid} + \omega_i C_i v_{Liq} \tag{3}$$

$$C_i \frac{dv_{Liq}}{dt} = i_{iq} - i_{Liq} - \omega_i C_i v_{Lid} \tag{4}$$

where ω_i is the angular frequency of each inverter and the inverter voltages v_{id} and v_{iq} represent the control inputs.

The main task in this paper is to design a droop controller for paralleled three-phase inverters with current-limiting and closed-loop system stability properties. In [21], a droop controller that can ensure a current limitation for a single-phase grid-connected inverter at all times is proposed. This is accomplished through the BIC [22], which ensures that the virtual resistance leading to the current-limiting property is bounded in a range set by the control operator. However, the same control structure can not be applied to inverters operating in parallel where proportional power sharing is required while the analysis presented in [21] assumes a stiff grid, which is not true for islanded microgrids. Hence, the closed-loop system stability in the absence of a stiff grid needs to be examined. Moreover, the SRF should be utilized since the abc quantities are transformed into dc at the steady state, and thus the computational burden is reduced for the controller implementation. In the sequel of this paper, a controller that deals with all the above is proposed.

III. THE PROPOSED CURRENT-LIMITING DROOP CONTROLLER

The proposed controller for each inverter operating in parallel takes the form

$$v_{id} = v_{Lid} + \frac{(w_i - w_{mi})^2}{\Delta w_{mi}^2} (E_d - w_i i_{id}) - \omega_i L_i i_{iq} \tag{5}$$

$$v_{iq} = v_{Liq} - w_i^{min} i_{iq} + \omega_i L_i i_{id} \tag{6}$$

where E_d is the nominal load voltage on d axis which for the used SRF transformation ($\theta_\alpha = 90^o$) is derived as $E_d = \sqrt{2} E_{rms}$ with E_{rms} being a constant representing the nominal RMS load voltage. The term $\frac{(w_i - w_{mi})^2}{\Delta w_{mi}^2}$ is used
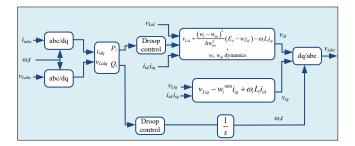
Fig. 2. Implementation of the proposed controller

Fig. 3. Equivalent closed-loop system

in order to achieve a smooth connection thus avoiding any possible overvoltage that could arise due to the constant parameter E_d. The terms $\omega_i L_i i_{iq}$ and $\omega_i L_i i_{id}$ represent the decoupling terms and w_i^{min} is the minimum value of the virtual resistance w_i applied to the d axis, which changes according to the nonlinear expressions

$$\dot{w_i} = -c_{wi} f_i(P_i) w_{qi}^2 \quad (7)$$

$$\dot{w_{qi}} = \frac{c_{wi}(w_i - w_{mi})w_{qi}}{\Delta w_{mi}^2} f_i(P_i) - k_w\left(\frac{(w_i - w_{mi})^2}{\Delta w_{mi}^2} + w_{qi}^2 - 1\right)w_{qi} \quad (8)$$

where c_{wi} and k_w are positive constants. Through this structure w_i is bounded in the range $\left[w_i^{min}, w_i^{max}\right] = [w_{mi} - \Delta w_{mi}, w_{mi} + \Delta w_{mi}]$ while $w_{mi} = \frac{w_i^{min} + w_i^{max}}{2}$ and $\Delta w_{mi} = \frac{w_i^{max} - w_i^{min}}{2}$. For more information the reader is referred to [21]. The function $f_i(P_i)$ inherits the droop control expression, which is applied in the proposed controller through the virtual resistance dynamics and takes the form

$$f_i(P_i) = E_{rms} - V_L - n_{pi} P_i \quad (9)$$

where $P_i = \frac{3}{2}(v_{Lid} i_{id} + v_{Liq} i_{iq})$. The reactive power droop control is applied through the SRF transformation and is described from

$$\omega_i = \omega^* + m_{qi} Q_i \quad (10)$$

where $Q_i = \frac{3}{2}(v_{Liq} i_{id} - v_{Lid} i_{iq})$. In the droop expressions, n_{pi} represents the real power droop coefficient, m_{qi} represents the reactive power droop coefficient while V_L is the RMS load voltage which is calculated from $\sqrt{2}V_L = \sqrt{v_{Lid}^2 + v_{Liq}^2}$ and ω^* is the nominal angular frequency. One can see that real power droop control is applied through the d component of the inverter voltage (which is a control input of the system) and reactive power droop is applied through the angular frequency dynamics. The $P \sim V$, $Q \backsim -\omega$ droop expressions are used in this paper since the universal droop controller from [9] is adopted. The implementation of the proposed controller is shown in Fig. 2. As highlighted before, for the virtual resistance dynamics in (7)-(8), the BIC setup from [22] is employed to guarantee the boundedness of the virtual resistance w_i. This property will lead to the boundedness of the inverter current for every three-phase inverter as it will be analytically shown in the analysis that follows.
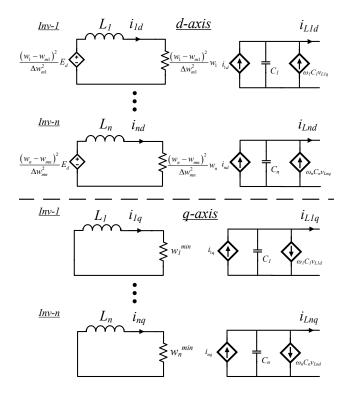
IV. CLOSED-LOOP SYSTEM STABILITY ANALYSIS

A. Current-limiting property

Applying the proposed controller (5)-(6) into the system dynamics (1)-(4), the closed-loop system takes the form depicted in Fig. 3. The inverter current dynamics are

$$L_i \frac{di_{id}}{dt} = \frac{(w_i - w_{mi})^2}{\Delta w_{mi}^2}(E_d - w_i i_{id}) \quad (12)$$

$$L_i \frac{di_{iq}}{dt} = -w_i^{min} i_{iq}. \quad (13)$$

This also verifies that the steady-state currents take the values $i_{ide} = \frac{E_d}{w_i}$ and $i_{iqe} = 0$. Now, let us consider the Lyapunov function candidate

$$V = \frac{1}{2}L_i i_{id}^2 + \frac{1}{2}L_i i_{iq}^2,$$

which represents the energy stored in each inductor. Its time derivative takes the form

$$\dot{V} = \frac{(w_i - w_{mi})^2}{\Delta w_{mi}^2}\left(E_d i_{id} - w_i i_{id}^2\right) - w_i^{min} i_{iq}^2$$

$$\leq \frac{(w_i - w_{mi})^2}{\Delta w_{mi}^2}\left([E_d\ 0]\begin{bmatrix} i_{id} \\ i_{iq} \end{bmatrix} - w_i^{min}\left(i_{id}^2 + i_{iq}^2\right)\right)$$

$$\leq \frac{(w_i - w_{mi})^2}{\Delta w_{mi}^2}\left(-w_i^{min}\|I_i\|_2^2 + \|E\|_2\|I_i\|_2\right)$$

where $I_i = [i_{id}\ i_{iq}]^T$ and $E = [E_d\ 0]^T$. Thus, it is concluded that

$$\dot{V} < 0, \forall \|I_i\|_2 > \frac{\|E\|_2}{w_i^{min}}. \quad (14)$$

$$A_T = \begin{bmatrix}
-\frac{\epsilon^2 w_{1e}}{\Delta w_{m1}^2 L_1} & 0 & 0 & 0 & 0 & 0 & -\frac{\epsilon^2 i_{1de}}{\Delta w_{m1}^2 L_1} & 0 \\
0 & -\frac{\zeta^2 w_{2e}}{\Delta w_{m2}^2 L_2} & 0 & 0 & 0 & 0 & 0 & -\frac{\zeta^2 i_{2de}}{\Delta w_{m2}^2 L_2} \\
0 & 0 & -\frac{w_1^{min}}{L_1} & 0 & 0 & 0 & 0 & 0 \\
0 & 0 & 0 & -\frac{w_2^{min}}{L_2} & 0 & 0 & 0 & 0 \\
\frac{\cos\delta_e}{C_1+C_2} & \frac{\cos\delta_e}{C_1+C_2} & -\frac{\sin\delta_e}{C_1+C_2} & -\frac{\sin\delta_e}{C_1+C_2} & -\frac{1}{R(C_1+C_2)} & \omega_0 & 0 & 0 \\
\frac{\sin\delta_e}{C_1+C_2} & \frac{\sin\delta_e}{C_1+C_2} & \frac{\cos\delta_e}{C_1+C_2} & \frac{\cos\delta_e}{C_1+C_2} & -\omega_0 & -\frac{1}{R(C_1+C_2)} & 0 & 0 \\
\frac{3}{2}c_{w1}n_{p1}\gamma w_{q1e}^2 & 0 & \frac{3}{2}c_{w1}n_{p1}\sigma w_{q1e}^2 & 0 & \alpha_1 c_{w1}w_{q1e}^2 & \beta_1 c_{w1}w_{q1e}^2 & 0 & 0 \\
0 & \frac{3}{2}c_{w2}n_{p2}\gamma w_{q2e}^2 & 0 & \frac{3}{2}c_{w2}n_{p2}\sigma w_{q2e}^2 & \alpha_2 c_{w2}w_{q2e}^2 & \beta_2 c_{w2}w_{q2e}^2 & 0 & 0
\end{bmatrix} \tag{11}$$

Furthermore, taking into account the relation between the dq quantities with the RMS values

$$\|I_i\|_2 = \sqrt{i_{id}^2 + i_{iq}^2} = \sqrt{2}I_{irms}$$

$$\|E\|_2 = \sqrt{E_d^2} = E_d = \sqrt{2}E_{rms}$$

and since (14) holds true, then if initially $I_{irms}(0) \leq \frac{E_{rms}}{w_{min}}$, then

$$I_{irms}(t) \leq \frac{E_{rms}}{w_i^{min}}, \forall t \geq 0. \tag{15}$$

By selecting $w_i^{min} = \frac{E_{rms}}{I_{irms}^{max}}$ then $I_{irms}(t) \leq I_{irms}^{max}, \forall t \geq 0$ for a given maximum value of the RMS current I_{irms}^{max}. Since the boundedness in (15) is proven independently from the load voltage or frequency, the RMS inverter current can reach but never exceed its set maximum value, for any $t > 0$. According to this, the controller variable I_{irms}^{max} can be selected by the control operator in order to ensure a current limitation under this threshold value at all times, even under transients and for any type of load.

B. Small-signal stability analysis

Although a current-limiting property is guaranteed for every inverter, the stability of multiple inverters operating in parallel has not been proven yet. In order to evaluate the proposed controller in terms of the closed-loop system stability, an exemplary case of two three-phase inverters operating in parallel is considered for simplicity, although the same approach can be extended to multiple parallel inverters. The state vector of the closed-loop system when considering two parallel three-phase inverters feeding a resistive load is $x = [i_{1d}\, i_{2d}\, i_{1q}\, i_{2q}\, v_{Ld}\, v_{Lq}\, w_1\, w_2\, w_{q1}\, w_{q2}]^T$. Note that, as shown in Fig. 1, both inverters have access to the common load voltage and additionally i_{iqe} becomes zero at the steady-state. This means that at the steady-state, when power sharing is achieved and all frequencies have been synchronized, the dq axes of every inverter will be aligned to each other and will have an angle difference δ_e compared to the global reference frame, where v_{Ld} and v_{Lq} is calculated. At this global reference frame, the capacitor voltage is aligned on d axis ($v_{Lqe} = 0$). Then, the Jacobian matrix of the closed-loop system takes the form

$$A = \begin{bmatrix} A_T & 0_{8\times1} & 0_{8\times1} \\ A_1 & -2k_w w_{q1e}^2 & 0 \\ A_2 & 0 & -2k_w w_{q2e}^2 \end{bmatrix}.$$
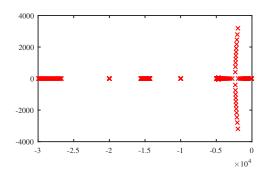

Fig. 4. Spectrum of the closed-loop system eigenvalues as a function of n_{pi} : $\frac{0.03E_{rms}}{S_{maxi}} < n_{pi} < \frac{0.3E_{rms}}{S_{maxi}}$
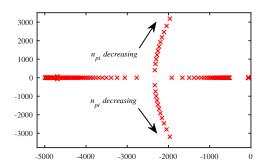

Fig. 5. Spectrum of the closed-loop system eigenvalues close to the imaginary axis as a function of n_{pi} : $\frac{0.03E_{rms}}{S_{maxi}} < n_{pi} < \frac{0.3E_{rms}}{S_{maxi}}$

However, since in the bounded range of operation it holds $w_i \in \left(w_i^{min}, w_i^{max}\right)$, then for any equilibrium point x_e with $w_{q1e}, w_{q2e} \in (0, 1]$, the values $-2k_w w_{q1e}^2$ and $-2k_w w_{q2e}^2$ are always negative. Thus, all the eigenvalues of the closed-loop system will be negative if all the eigenvalues of the matrix A_T, analytically shown in (11), have negative real parts. To facilitate the representation of A_T, the following notations are considered: $\alpha_i = \frac{3}{2}n_{pi}i_{ide}\cos\delta_e + 1/\sqrt{2}$, $\beta_i = \frac{3}{2}n_{pi}i_{ide}\sin\delta_e$, $\gamma = v_{Lde}\cos\delta_e$, $\sigma = -v_{Lde}\sin\delta_e$, $\epsilon = (w_{1e} - w_{m1})$ and $\zeta = (w_{2e} - w_{m2})$. In order to perform a root-locus analysis for the matrix A_T, the equilibrium point of the closed-loop system, $x_e = [i_{1de}\, i_{2de}\, i_{1qe}\, i_{2qe}\, v_{Lde}\, v_{Lqe}\, w_{1e}\, w_{2e}\, w_{q1e}\, w_{q2e}]^T$ needs to be identified. This is possible through solving the system of equations (12)-(13), (3)-(4) and (9)-(10) while ω_0 represents the system steady-state frequency at each equilibrium point when considering that synchronization has been achieved, as in [12]. The droop coefficients are calculated from the formulas $n_{pi} = 0.09\frac{E_{rms}}{S_{maxi}}$ and $m_{qi} = 0.01\frac{\omega^*}{S_{maxi}}$. Therefore through

root-locus analysis, the closed-loop system stability for the case of two parallel inverters feeding a resistive load and equipped with the proposed controller can be examined, while the considered system parameters are given in Table I.
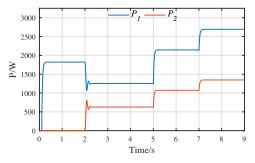
In Fig. 4, the eigenvalues of the closed-loop system for a resistive load with $R = 10\Omega$ are depicted for a real power droop percentage (n_{pi}) between 3% and 30%. Since all the eigenvalues have negative real part, it is concluded that the closed-loop system is stable around the considered equilibrium point. Furthermore, in Fig. 5, the trajectory of the eigenvalues that are closer to the imaginary axis is depicted, where it can be understood that as n_{pi} gets lower values, eigenvalues tend more close to the unstable region.
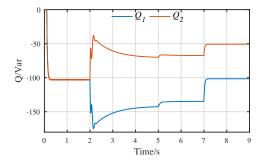
TABLE I
SYSTEM AND CONTROLLER PARAMETERS

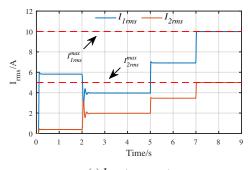| Parameters	Values	Parameters	Values
L_1, L_2	1.1 mH	C_1, C_2	10 μF
S_{max1}	3300 VA	S_{max2}	1650 VA
ω^*	2π x 50 rad/s	E_{rms}	110 V
n_{p1}	0.003	m_{q1}	0.000952
n_{p2}	0.006	m_{q2}	0.0019
I_{1rms}^{max}	10 A	I_{2rms}^{max}	5 A
I_{1rms}^{min}-I_{2rms}^{min}	0.14 A	k_w	1000
w_{m1}	394 Ω	w_{m2}	399 Ω

V. CONTROLLER VERIFICATION

To validate the performance of the proposed controller, two parallel three-phase inverters connected to a common load bus, as depicted in Fig. 1, are simulated in the Matlab/Simulink environment. The system and controller parameters are given in Table I. Initially both inverters do not feed the load since their switches are open while at 0.1s, the first inverter is connected to the load which initially has the value $R = 18\Omega$. As it can be seen in Fig. 6a, the first inverter quickly regulates its output real power P_1 in order to achieve a load voltage close to its nominal value through droop control. Similarly, in Fig. 6b, it is shown that reactive power is accordingly injected to regulate load frequency close to the nominal frequency. The load bus voltage V_L and frequency f are regulated close to their nominal values as depicted in Figures 7b and 7c, respectively. At 2s, the second inverter is connected to the common load bus and since a 2:1 power sharing ratio is desired according to the capacity of the inverters, both real and reactive power are shared proportionally so that $P_1 = 2P_2$ and $Q_1 = 2Q_2$, as it can be observed in Figures 6a and 6b. To accomplish this, P_1 is reduced, so that both power inverters are stressed equally whilst as shown in Fig. 7b, V_L is now regulated to a higher value which can be understood from (9). At 5s, a load change is experienced and the total load is driven to $R = 10\Omega$. As shown in Figures 6a and 6b, the inverters modify their response whilst the power sharing remains accurate. At 7s, an even higher demand occurs leading the common load to $R = 6\Omega$ which demands a power greater than the total capacity of the two parallel inverters $S_{max1} + S_{max2}$. However, according to the theory presented in this paper, at that time both controller states w_1 and w_2 are

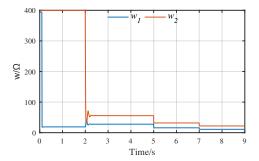(a) Real Power

(b) Reactive Power

(c) Inverter currents

Fig. 6. Response of two three-phases inverters operating in parallel: Real power, Reactive power and Inverter currents
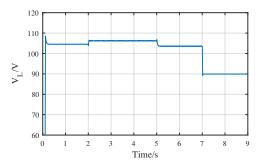
driven to their minimum values (11Ω and 22Ω respectively, as shown in Fig. 7a) thus, limiting the inverter currents I_{1rms} and I_{2rms} to their maximum values as shown in Fig. 6c. Hence, the DERs are protected from overcurrents while the load bus voltage V_L drops significantly, since priority is given to protecting the inverter devices. The presented simulation results verify the proportional power sharing and current-limiting capabilities of the proposed controller.

VI. CONCLUSIONS

In this paper, a new current-limiting droop controller is proposed for three-phase inverters operating in parallel. The proportional power sharing property of the inverters operating in parallel is guaranteed through the widely used droop control. The desired current-limiting property is proven through nonlinear analysis of the closed-loop system which leads to the boundedness of each inverter current under a threshold value at all times, even under transients. Moreover, the stable operation

(a) Controller states w_1 and w_2

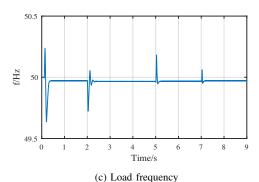(b) Load RMS voltage

(c) Load frequency

Fig. 7. Response of two three-phases inverters operating in parallel: Controller states, Load voltage and Load frequency

of two inverters operating in parallel is guaranteed through the performed small-signal stability analysis. The proposed control approach is further validated through extended simulation results.

ACKNOWLEDGMENT

REFERENCES

[1] P. Piagi and R. H. Lasseter, "Autonomous control of microgrids," in *2006 IEEE Power Engineering Society General Meeting*, 2006, pp. 1–8.
[2] N. Hatziargyriou, *Microgrids: Architectures and Control*. Hoboken, NJ, USA: Wiley, 2014.
[3] D. E. Olivares, A. Mehrizi-Sani, A. H. Etemadi, C. A. Canizares, R. Iravani, M. Kazerani, A. H. Hajimiragha, O. Gomis-Bellmunt, M. Saeedifard, R. Palma-Behnke, G. A. Jimenez-Estevez, and N. D. Hatziargyriou, "Trends in microgrid control," *IEEE Transactions on Smart Grid*, vol. 5, no. 4, pp. 1905–1919, July 2014.
[4] J. Guerrero, M. Chandorkar, T. Lee, and P. Loh, "Advanced control architectures for intelligent microgrids-Part I: Decentralized and hierarchical control," *IEEE Trans. Ind. Electron.*, vol. 60, no. 4, pp. 1254–1262, Apr. 2013.
[5] Y. Xue and J. M. Guerrero, "Smart inverters for utility and industry applications," in *Proceedings of PCIM Europe 2015; International Exhibition and Conference for Power Electronics, Intelligent Motion, Renewable Energy and Energy Management*, May 2015, pp. 1–8.
[6] M. Chandorkar, D. Divan, and R. Adapa, "Control of parallel connected inverters in standalone ac supply systems," *IEEE Transactions on Industry Applications*, vol. 29, no. 1, pp. 136–143, Jan. 1993.
[7] J. M. Guerrero, J. Matas, L. G. de Vicuna, M. Castilla, and J. Miret, "Decentralized control for parallel operation of distributed generation inverters using resistive output impedance," *IEEE Transactions on Industrial Electronics*, vol. 54, no. 2, pp. 994–1004, April 2007.
[8] Y. Sun, X. Hou, J. Yang, H. Han, M. Su, and J. M. Guerrero, "New perspectives on droop control in ac microgrid," *IEEE Transactions on Industrial Electronics*, vol. 64, no. 7, pp. 5741–5745, July 2017.
[9] Q. C. Zhong and Y. Zeng, "Universal droop control of inverters with different types of output impedance," *IEEE Access*, vol. 4, pp. 702–712, 2016.
[10] C. C. Chang, D. Gorinevsky, and S. Lall, "Stability analysis of distributed power generation with droop inverters," *IEEE Transactions on Power Systems*, vol. 30, no. 6, pp. 3295–3303, Nov 2015.
[11] Y. Song, D. J. Hill, T. Liu, and Y. Zheng, "A distributed framework for stability evaluation and enhancement of inverter-based microgrids," *IEEE Transactions on Smart Grid*, vol. 8, no. 6, pp. 3020–3034, Nov 2017.
[12] N. Pogaku, M. Prodanovic, and T. Green, "Modeling, Analysis and Testing of Autonomous Operation of an Inverter-Based Microgrid," *IEEE Trans. Power Electron.*, vol. 22, no. 2, pp. 613–625, 2007.
[13] X. Zhao, J. M. Guerrero, M. Savaghebi, J. C. Vasquez, X. Wu, and K. Sun, "Low-voltage ride-through operation of power converters in grid-interactive microgrids by using negative-sequence droop control," *IEEE Transactions on Power Electronics*, vol. 32, no. 4, pp. 3128–3142, April 2017.
[14] R. Majumder, B. Chaudhuri, A. Ghosh, R. Majumder, G. Ledwich, and F. Zare, "Improvement of stability and load sharing in an autonomous microgrid using supplementary droop control loop," *IEEE Transactions on Power Systems*, vol. 25, no. 2, pp. 796–808, May 2010.
[15] T. Hosseinimehr, F. Shahnia, and A. Ghosh, "Dynamic power sharing control among converter-interfaced ders in an autonomous microgrid," in *2015 IEEE Eindhoven PowerTech*, June 2015, pp. 1–6.
[16] H. Xin, L. Huang, L. Zhang, Z. Wang, and J. Hu, "Synchronous instability mechanism of p-f droop-controlled voltage source converter caused by current saturation," *IEEE Transactions on Power Systems*, vol. 31, no. 6, pp. 5206–5207, Nov 2016.
[17] Z. Shuai, C. Shen, X. Yin, X. Liu, and Z. J. Shen, "Fault analysis of inverter-interfaced distributed generators with different control schemes," *IEEE Transactions on Power Delivery*, vol. 33, no. 3, pp. 1223–1235, June 2018.
[18] A. D. Paquette and D. M. Divan, "Virtual impedance current limiting for inverters in microgrids with synchronous generators," *IEEE Transactions on Industry Applications*, vol. 51, no. 2, pp. 1630–1638, March 2015.
[19] N. Bottrell and T. C. Green, "Comparison of current-limiting strategies during fault ride-through of inverters to prevent latch-up and wind-up," *IEEE Trans. Power Electron.*, vol. 29, no. 7, pp. 3786–3797, 2014.
[20] X. Lu, J. Wang, J. M. Guerrero, and D. Zhao, "Virtual-impedance-based fault current limiters for inverter dominated ac microgrids," *IEEE Transactions on Smart Grid*, vol. 9, no. 3, pp. 1599–1612, May 2018.
[21] Q. C. Zhong and G. C. Konstantopoulos, "Current-limiting droop control of grid-connected inverters," *IEEE Transactions on Industrial Electronics*, vol. 64, no. 7, pp. 5963–5973, July 2017.
[22] G. C. Konstantopoulos, Q. C. Zhong, B. Ren, and M. Krstic, "Bounded integral control of input-to-state practically stable nonlinear systems to guarantee closed-loop stability," *IEEE Transactions on Automatic Control*, vol. 61, no. 12, pp. 4196–4202, Dec 2016.
[23] C. T. Rim, D. Y. Hu, and G. H. Cho, "Transformers as equivalent circuits for switches: general proofs and d-q transformation-based analyses," *IEEE Transactions on Industry Applications*, vol. 26, no. 4, pp. 777–785, Jul 1990.
[24] B. K. Bose, *Modern Power Electronics and AC Drives*. Prentice Hall PTR, 2002.